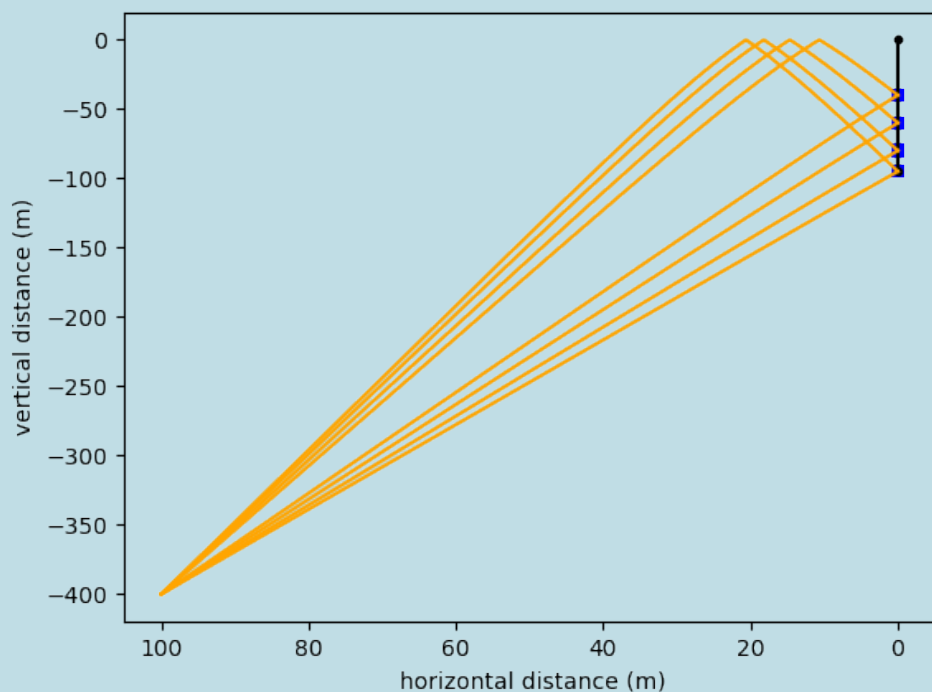# Radio detection of high energy neutrinos in the Greenland icecap

Arthur Adriaens

Department of Physics and Astronomy

Promotor: Prof. dr. Dirk Ryckbosch   Dirk.Ryckbosch@ugent.be

Accompanist: Bob Oeyen   Bob.Oeyen@ugent.be

Master's dissertation submitted in partial fulfilment of the requirements for the degree of master in Physics and Astronomy

CONTENTS

CHAPTER

1

FOREWORD

1.1 Abstract: English

The Radio Neutrino Observatory in Greenland - RNO-G - is under construction at Summit Station in Greenland to search for neutrinos of several PeV energy up to the Eev range. It's a mid-scale, discovery phase, extremely high-energy neutrino telescope that will probe the astrophysical neutrino flux at energies beyond the reach of IceCube. More particularly if will make it possible to reach the next major milestone in astroparticle physics: the discovery of cosmogenic neutrinos. All simulations carried out within this work were made with the three

programs

- NuRadioMC

- radiotools

- RadioPropa

whom are free to download on github. The projects built over the course of this thesis were the "Hybrid minimizer": a new algorithm for finding the path of a neutrino interaction to the detector in complex ice models and (...)

1.2 Abstract: Nederlands

De *Radio Neutrino Observatory in Greenland* - RNO-G - is een detector die momenteel onder constructie is in Groenland. Deze detector heeft als doel het vinden van neutrino's met energieën van enkele PeV tot in het EeV gebied. Deze extreem hoge energy neutrino telescoop zal astrofysische neutrinos zoeken op energieën waar icecube te klein voor is. Het zal ook het vinden van cosmogenische neutrinos mogelijk maken. Alle simulaties werden mogelijk gemaakt door de volgende programmas:

- NuRadioMC

- radiotools

- RadioPropa

Dewelke te downloaden zijn op github De projecten die tot completie zijn gebracht over deze master thesis waren de *Hybrid minimizer*: een algoritme gemaakt met als doel het snel vinden van een pad vanuit de interactievertex tot de detector in complexe ijsmodellen en (...)

2

BACKGROUND: NEUTRINOS

2.1 Electroweak interaction

$$\mathcal{L}_{SM} = -\frac{1}{4}F_{\mu\nu}F^{\mu\nu}$$
$$+ i\bar{\psi}\slashed{D}\psi + h.c$$
$$+ \psi_i y_{ij}\psi_j\phi + h.c$$
$$+ |\mathcal{D}_\mu\phi|^2 - V(\phi)$$

Above we see the standard model lagrangian density, consisting of the following parts: at the top the Generalized maxwell lagrangian, the second line being the generlaized lorentz force, the third line the yukawa couplings (rest mass[1] via higgs boson and massless quark&lepton field coupling) and the last line responsible for the spontaneous symmetry breaking giving rise to the rest mass via the Brout Englert Higgs mechanism. We'll mostly concern ourselves with the second part.

2.1.1 History

Fermi realised a quantitatively good local field theory for the β-decay in 1934 based on the idea of the following interaction:

$$n \to p + e^- + \bar{\nu} \tag{2.1}$$

i.e

This 4-fermion interaction is however not renormalizable, meaning that it will be incorrect for sufficiently high energies. As the lagrangian density would look like

$$\mathcal{L}_{int}^F = -G_F(\bar{\psi}_p\gamma_\mu\psi_n)(\bar{\psi}_e\gamma^\mu\psi_\nu) + h.c \tag{2.2}$$

And indeed, from dimensionality analysis we see that, as $[\psi] = [L]^{-3/2}$, we get that from $[\mathcal{L}_{int}] = [L]^{-4}$, $[G_F] = [L]^2 = [\Lambda]^{-2}$

---

[1]nearly all the mass observed in e.g nuclei actually comes from binding energy.
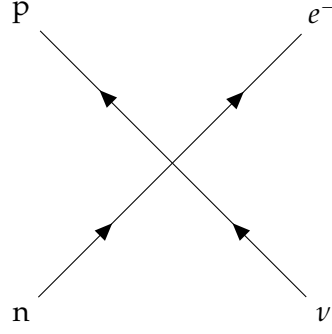
This interaction lagrangian density also doens't explain how this weak interaction violates parity, as was observed in the $\tau - \theta$ puzzle where it has become apparent that the weak interaction only couples to the left handed part of lepton- and baryon fields. Everything was finally explained using the V-A model, which we'll get to shortly.

2.1.2 Chiral gauge theories

Let's first give a quick example on how parity can be violated in a gauge theory; let's define the operators

$$P_R = \frac{1}{2}(1 + \gamma_5) \quad P_L = \frac{1}{2}(1 - \gamma_5) \tag{2.3}$$

with

$$\gamma_5 = i\gamma_0\gamma_1\gamma_2\gamma_3 \tag{2.4}$$

And with this defining

$$\psi_R := P_R\psi \quad \psi_L := P_L\psi \tag{2.5}$$

Now starting from the simple kinetic lagrangian density:

$$\mathcal{L} = i\bar{\psi}\!\!\not{\partial}\psi - m\bar{\psi}\psi \tag{2.6}$$

We can re-write this as follows:

$$\mathcal{L} = i\bar{\psi}_R\!\!\not{\partial}\psi_R + i\bar{\psi}_L\!\!\not{\partial}\psi_L - m\bar{\psi}_R\psi_L - m\bar{\psi}_L\psi_R \tag{2.7}$$

Now we wish to have gauge invariance over the whole lagrangian density, i.e having

$$\psi_R(x) \rightarrow \psi'_R(x) = e^{iq_Rf(x)}\psi_R(x) \tag{2.8}$$

$$\psi_L(x) \rightarrow \psi'_L(x) = e^{iq_Lf(x)}\psi_L(x) \tag{2.9}$$

Now in the maxwellian term of the standard model, as

$$F_{\mu\nu} = \partial_\mu A_\nu - \partial_\mu A_\nu \tag{2.10}$$

The A field has a gauge transform of the form

$$A_\mu(x) \rightarrow A'_\mu(x) = A_\mu(x) - \partial_\mu f(x) \tag{2.11}$$

Thus if we define the covariant derivatives

$$\mathcal{D}_\mu\psi_R = \partial_\mu\psi_R + iq_R A_\mu\psi_R \tag{2.12}$$

$$\mathcal{D}_\mu\psi_L = \partial_\mu\psi_L + iq_L A_\mu\psi_L \tag{2.13}$$

We see that our lagrangian density

$$\mathcal{L} = i\bar{\psi}_R \slashed{D}\psi_R + i\bar{\psi}_L \slashed{D}\psi_L \tag{2.14}$$

Is gauge invariant. If you write this out you get

$$i\bar{\psi}\slashed{\partial}\psi - \frac{q_R + q_L}{2}\bar{\psi}\slashed{A}\psi - \frac{q_R - q_L}{2}\bar{\psi}\slashed{A}\gamma_5\psi \tag{2.15}$$

The rightmost term is a pseudoscalar, we thus see that this system breaks parity invariance if $q_L \neq q_R$. This is a crude form of the V-A theory.

2.1.3 $SU(2) \to SU(2)_L \times U(1)_Y$

We'll now quickly derive and discuss the weak interaction looking at a 2x2 constant $\mathbb{C}$ transformation

$$\Psi(x) \to M\Psi(x) \tag{2.16}$$

$$\bar{\Psi}(x) \to \bar{\Psi}(x)M^\dagger \tag{2.17}$$

We want the lagrangian density to be gauge invariant meaning that we wish them to obey

$$M^\dagger M = \mathbb{1}_{2x2} \tag{2.18}$$

i.e we want them to be unitary, aside from this we also choose $det(M) = 1$ restricting ourselves to the special unitary 2D matrices (the SU(2) group), we get that if we take a look at the kinetic lagrangian density:

$$\mathcal{L} = i\bar{\Psi}\slashed{\partial}\Psi - m\bar{\Psi}\Psi \tag{2.19}$$

requiring invariance under the previously mentioned transformation, calculating we have that:

$$\partial_\mu \Psi \to \partial_\mu(M\Psi) = M(\partial_\mu\Psi + M^{-1}\partial_\mu M\Psi) \tag{2.20}$$

Now

$$(M^{-1}\partial_\mu M)^\dagger = \partial_\mu M^\dagger (M^{-1})^\dagger = \partial_\mu M^{-1}M \tag{2.21}$$

Due to them being from the SU(2) group, now as $M^{-1}M = \mathbb{1}_{2x2}$:

$$\partial_\mu(M^{-1}M) = 0 \implies \partial_\mu M^{-1}M = -M^{-1}\partial_\mu M \tag{2.22}$$

i.e $M^{-1}\partial_\mu M$ is anti-hermitian, now

$$\frac{\delta det(M)}{det(M)} = tr(M^{-1}\delta M) \tag{2.23}$$

$$\frac{\partial_\mu det(M)}{det(M)} = tr(M^{-1}\delta M) \tag{2.24}$$

The left side is zero as $det(M) = 0$, thus $M^{-1}\partial_\mu M$ is traceless and anti-hermitian, meaning that to make the lagrangian density gauge invariant under $SU(2)$, we can define the covariant derivative

$$\mathcal{D}_\mu \Psi = \partial_\mu \Psi + igW_\mu \Psi \tag{2.25}$$

With W_μ a traceless hermitian 2x2 matrix of gauge fields and $g \in \mathbb{R}$ a coupling constant. Now as is well know the complete basis of 2x2 hermitian traceless matrices are the Pauli matrices

$$\sigma_1 = \begin{pmatrix} 0 & 1 \\ 1 & 0 \end{pmatrix} \quad \sigma_2 = \begin{pmatrix} 0 & -i \\ i & 0 \end{pmatrix} \quad \sigma_3 = \begin{pmatrix} 1 & 0 \\ 0 & -1 \end{pmatrix} \tag{2.26}$$

meaning we can construct the gauge fields as

$$W_\mu = \frac{1}{2}\sum_{a=1}^{3} W_\mu^a(x)\sigma_a = \frac{1}{2}\begin{pmatrix} W_\mu^3 & W_\mu^1 - iW_\mu^2 \\ W_\mu^1 + iW_\mu^2 & -W_\mu^3 \end{pmatrix} \tag{2.27}$$

The lagrangian density then becomes

$$\mathcal{L} = i\bar{\Psi}\slashed{\partial}\Psi - m\bar{\Psi}\Psi - g\bar{\Psi}\slashed{W}\Psi := \mathcal{L}_0 + \mathcal{L}_I \tag{2.28}$$

I.e we get an extra interaction term. Now defining

$$W_\mu := \frac{1}{\sqrt{2}}(W_\mu^1 - iW_\mu^2) \tag{2.29}$$

$$W_\mu^\dagger := \frac{1}{\sqrt{2}}(W_\mu^1 + iW_\mu^2) \tag{2.30}$$

The interaction lagrangian density becomes

$$\mathcal{L}_I = -\frac{g}{2}(\bar{\psi}_1, \bar{\psi}_2)\begin{pmatrix} \slashed{W}^3 & \sqrt{2}\slashed{W} \\ \sqrt{2}\slashed{W}^\dagger & -\slashed{W}^3 \end{pmatrix}\begin{pmatrix} \psi_1 \\ \psi_2 \end{pmatrix} \tag{2.31}$$

$$= -\frac{g}{2}\bar{\psi}_1\slashed{W}^3\psi_1 + \frac{g}{2}\bar{\psi}_2\slashed{W}^3\psi_2 \tag{2.32}$$

$$-\frac{g}{\sqrt{2}}\bar{\psi}_1\slashed{W}\psi_2 + \frac{g}{\sqrt{2}}\bar{\psi}_2\slashed{W}^\dagger\psi_1 \tag{2.33}$$

I.e a flavour changing part and a non-flavour changing part. If we now set up this system with the vector

$$\Psi_\ell^L = \begin{pmatrix} \nu_l^L \\ \ell^L \end{pmatrix} \tag{2.34}$$

With also a U(1) transformation:

$$\Psi_\ell^L \to \Psi_\ell^{L'}(x) = M(x)e^{ig'q\beta(x)}\Psi_\ell^L(x) \tag{2.35}$$

Introducing the U(1) gauge field B_μ that transforms as in equation 2.11 we see that the covariant derivative needs to be defined as

$$\mathcal{D}_\mu\Psi_\ell^L = \partial_\mu\Psi_\ell^L + ig\hat{W}_\mu\Psi_\ell^L + ig'qB_\mu\Psi_\ell^L \tag{2.36}$$

Yielding an interaction lagrange density of the form

$$\mathcal{L}_I = \sum_\ell -g\bar{\Psi}_\ell^L\slashed{\hat{W}}\Psi_\ell^L - g'q\bar{\Psi}_\ell^L\slashed{B}\Psi_\ell^L \tag{2.37}$$

And after introducing the weak mixing angle (Glashow):

$$W_\mu^3 = \sin(\theta_W)A_\mu + \cos(\theta_W)Z_\mu \tag{2.38}$$

$$B_\mu = \cos(\theta_W)A_\mu + \sin(\theta_W)Z_\mu \tag{2.39}$$

We can go ahead and find our interaction lagrangian density for the photon field A_μ, the W-boson field W_μ and the Z-boson field Z_μ. Then an analogous analysis can be done for the quark sector and with that we'll have fully developed the electroweak theory[2] , thus finding the most important (for our discussion) interactions that can happen with neutrinos:

$$\mathcal{L}_I^\nu = \sum_l -\frac{g}{2\sqrt{2}}\bar{\nu}_l\slashed{W}(1-\gamma_5)l - \frac{g}{2\sqrt{2}}\bar{l}\slashed{W}^\dagger(1-\gamma_5)\nu_l \tag{2.40}$$

---

[2]note that this can be further generalized to arrive at cubic and quartic couplings e.g WWWW couplings which I won't go into here as it isn't relevant for this discussion, the symmetry breaking needed to give mass to the bosons also won't be discussed

And the production/annihilation mechanisms of $W/W^{\dagger}$ bosons from the quark sector:

$$\mathcal{L}_Q = \sum_j \bar{Q}_j i \not{D} Q_j \tag{2.41}$$

We can equate W with W^- and $W^{\dagger}$ with W^+. Here are some diagramattic exaples of possible interactions which you can conclude from those interaction lagrangian densities[3]:
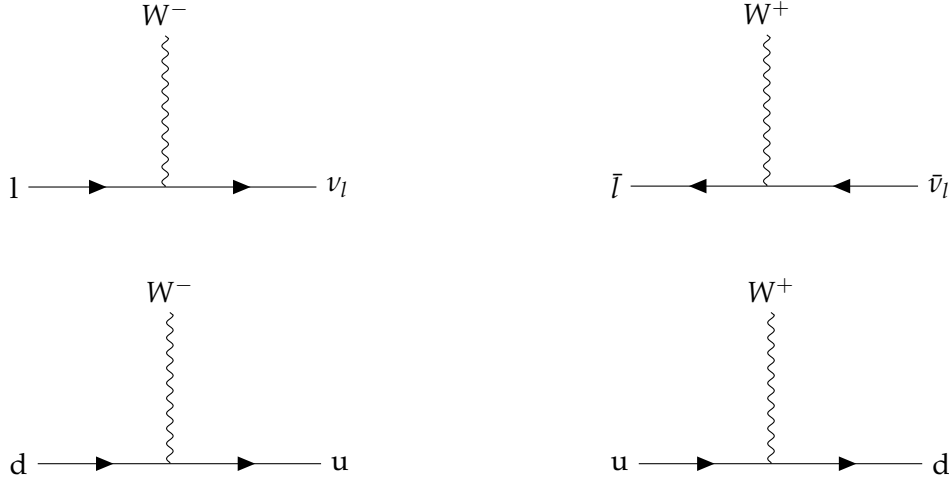
Combining some of these diagrams we can re-write Fermi's interaction in a renormalizable interaction:
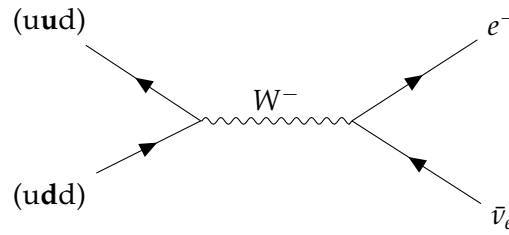
2.2 Do neutrinos have mass?

Neutrinos get produced through the following ways in the nucleus of our star:
pp − cycle

$$p + p \rightarrow D + e^+ + \nu_e \tag{2.42}$$
$$D + p \rightarrow {}^3\text{He} + \gamma \tag{2.43}$$
$${}^3\text{He} + {}^3\text{He} \rightarrow {}^4\text{He} + p + p \tag{2.44}$$

boron − cycle

$${}^4\text{He} + {}^3\text{He} \rightarrow {}^7\text{Be} + \gamma \tag{2.45}$$
$${}^7\text{Be} + p \rightarrow {}^8\text{B} + \gamma \tag{2.46}$$
$${}^8\text{B} \rightarrow {}^8\text{Be}^* + e^+ + \nu_e \tag{2.47}$$
$${}^8\text{Be}^* \rightarrow {}^4\text{He} + {}^4\text{He} \tag{2.48}$$

---
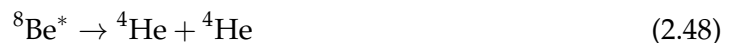
[3]with u, up-like quarks is meant, e.g charm, top. Analogously with d, down-like quarks

Be − capture

$$^7\text{Be} + e^- \rightarrow {}^7\text{Li} + \nu_e \tag{2.49}$$

pep

$$p + e^- + p \rightarrow D + \nu_e \tag{2.50}$$

Now with this and some information about the sun like the pressure and mass, the so-called "standard solar model" was made. This model predicted a certain amount of neutrinos to be hitting the earth from the previously mentioned thermonuclear fusion, it was however 3 times higher than the observed amount of neutrinos back at our planet. Through various experiments it became apparent that this was due to the various kind of neutrinos oscillating into each other, i.e 2/3 of the original electron neutrinos had oscillated into mu and tau neutrinos but for them to oscillate into eachother, they require mass:

2.2.1 neutrino oscillations

Let's only discuss this in 2D (this can easily be extended to 3D but we wish to be concise and only show the principle), define the mass-eigenstates as

$$|\nu_i(t)\rangle = |\nu_i\rangle \exp\{i(\mathbf{p}_i \cdot \mathbf{x} - E_i t)\} = |\nu_i\rangle e^{-i\phi} \tag{2.51}$$

Now let's say these are related to the lepton eigenstates as:

$$\begin{pmatrix} \nu_e \\ \nu_\mu \end{pmatrix} = \begin{pmatrix} \cos\theta & \sin\theta \\ -\sin\theta & \cos\theta \end{pmatrix} \begin{pmatrix} \nu_1 \\ \nu_2 \end{pmatrix} \tag{2.52}$$

Assume at $t = 0$ pure ν_e (starting at the sun core):

$$|\psi(0)\rangle = cos\theta \, |\nu_1\rangle + \sin\theta \, |\nu_2\rangle \tag{2.53}$$

At time T, at distance L

$$|\psi(L,T)\rangle = \cos\theta \, |\nu_1\rangle \, e^{-i\phi_1} + \sin\theta \, |\nu_2\rangle \, e^{-i\phi_2} \tag{2.54}$$

$$= (e^{-i\phi_1} \cos^2\theta + e^{-i\phi_2} \sin^2\theta) \, |\nu_e\rangle - (e^{-i\phi_1} - e^{-\phi_2}) \cos\theta \sin\theta \, |\nu_\mu\rangle \tag{2.55}$$

$$= e^{-i\phi_1} \left[\left(\cos^2\theta + e^{i\Delta\phi_{12}} \sin^2\theta \right) | \, \nu_e > \right. \tag{2.56}$$

$$\left. - \left(1 - e^{i\Delta\phi_{12}} \right) \cos\theta \sin\theta \, | \, \nu_\mu > \right] \tag{2.57}$$

$$:= c_e \, |\nu_e\rangle \, c_\mu \, |\nu_\mu\rangle \tag{2.58}$$

With

$$\Delta\phi_{12} = (E_1 - E_2) \, T - (p_1 - p_2) \, L \tag{2.59}$$

So the transition probability is

$$P(\nu_e \rightarrow \nu_\mu) = |\langle \nu_\mu | \psi(L,T)\rangle|^2 = c_\mu c_\mu^* = \sin^2(2\theta) \sin^2\left(\frac{\Delta\phi_{12}}{2}\right) \tag{2.60}$$

If you then proceed to do a full wave-packet propagation calculation you'll find

$$\Delta\phi_{12} \approx \frac{m_1^2 - m_2^2}{2p} L \tag{2.61}$$

I.e not only mass but difference in mass of the eigenstates is a requirement for oscillations to occur. In general

$$|\nu_\alpha\rangle = \sum_i U_{\alpha i} |\nu_i\rangle \tag{2.62}$$

With $U_{\alpha i}$ e.g the Pontecorvo-Maki-Nakagawa-Sakata (PMNS) matrix. This phenomenon has been observed e.g from the descrepency from the observed and expected neutrino events coming from a nuclear reactor [4]. Now the question remains, how do neutrinos get their mass (theoretically)?

2.2.2 See-saw mechanism

We can give neutrino's mass as with any other spinor throught Yukawa couplings and an extra term:

$$\mathcal{L} = i\bar{\nu}\slashed{\partial}\nu - m\bar{\psi}\nu - \frac{M}{2}(\bar{\nu}_R\nu_{Rc} + \bar{\nu}_{Rc}\nu_R) \tag{2.63}$$

More general, given a spinor ψ with the following Lagrange density:

$$\mathcal{L} = i\bar{\psi}\slashed{\partial}\psi - m\bar{\psi}\psi - \frac{M}{2}(\bar{\psi}_R\psi_{Rc} + \bar{\psi}_{Rc}\psi_R) \tag{2.64}$$

We can re-write this Lagrangian in terms of

$$\chi := \frac{1}{\sqrt{2}}(\psi_R + \psi_{Rc}) \tag{2.65}$$

$$\omega := \frac{1}{\sqrt{2}}(\psi_L + \psi_{Lc}) \tag{2.66}$$

by first identifying that

$$-\frac{M}{2}(\bar{\psi}_R\psi_{Rc} + \bar{\psi}_{Rc}\psi_R) \tag{2.67}$$

is equal to

$$-M\bar{\chi}\chi = -\frac{M}{2}(\bar{\psi}_R + \bar{\psi}_{Rc})(\psi_R + \psi_{Rc}) = -\frac{M}{2}(\bar{\psi}_R\psi_{Rc} + \bar{\psi}_{Rc}\psi_R) \tag{2.68}$$

Where we've used

$$\bar{\psi}_R\psi_R \equiv \psi_R^\dagger\gamma^0\psi_R \equiv P_R\psi^\dagger\gamma^0 P_R\psi = P_R P_L\psi^\dagger\gamma^0\psi = 0 \tag{2.69}$$

And next that in

$$i\bar{\psi}\slashed{\partial}\psi - m\bar{\psi}\psi = i\bar{\psi}_R\slashed{\partial}\psi_R + i\bar{\psi}_L\slashed{\partial}\psi_L - m\bar{\psi}_R\psi_L - m\bar{\psi}_L\psi_R \tag{2.70}$$

We can identify that

$$\bar{\chi}\slashed{\partial}\chi = \frac{1}{2}(\bar{\psi}_R\slashed{\partial}\psi_R + \bar{\psi}_{Rc}\slashed{\partial}\psi_{Rc}) = \bar{\psi}_R\slashed{\partial}\psi_R \tag{2.71}$$

$$\bar{\omega}\slashed{\partial}\omega = \bar{\psi}_L\slashed{\partial}\psi_L \tag{2.72}$$

Where we've done an integration by parts and used $\bar{\psi}_c\gamma_\mu\chi_c = -\bar{\chi}\gamma_\mu\psi$. We thus get:

$$\mathcal{L} = i\bar{\chi}\slashed{\partial}\chi + i\bar{\omega}\slashed{\partial}\omega - m\bar{\psi}_R\psi_L - m\bar{\psi}_L\psi_R - M\bar{\chi}\chi \tag{2.73}$$

And finally we notice that

$$\bar{\chi}\omega = \frac{1}{2}\left(\bar{\psi}_R\psi_L + \bar{\psi}_R\psi_{Lc} + \bar{\psi}_{Rc}\psi_L + \bar{\psi}_{Rc}\psi_{Lc}\right) \tag{2.74}$$

$$= \frac{1}{2}\left(\bar{\psi}_R\psi_L + \bar{\psi}_R\psi_{Lc} + \bar{\psi}_{Rc}\psi_L + \bar{\psi}_L\psi_R\right) \tag{2.75}$$

$$\bar{\omega}\chi = \frac{1}{2}\left(\bar{\psi}_L\psi_R + \bar{\psi}_{Lc}\psi_R + \bar{\psi}_L\psi_{Rc} + \bar{\psi}_{Lc}\psi_{Rc}\right) \tag{2.76}$$

$$= \frac{1}{2}\left(\bar{\psi}_L\psi_R + \bar{\psi}_{Lc}\psi_R + \bar{\psi}_L\psi_{Rc} + \bar{\psi}_R\psi_L\right) \tag{2.77}$$

As $\bar{\psi}_c\chi_c = \bar{\chi}\psi$. Summing these, we get:

$$\bar{\chi}\omega + \bar{\omega}\chi = \bar{\psi}_L\psi_R + \bar{\psi}_R\psi_L \tag{2.78}$$

$$+ \frac{1}{2}\left(\bar{\psi}_R\psi_{Lc} + \bar{\psi}_{Rc}\psi_L + \bar{\psi}_{Lc}\psi_R + \bar{\psi}_L\psi_{Rc}\right) \tag{2.79}$$

$$= \bar{\psi}_L\psi_R + \bar{\psi}_R\psi_L \tag{2.80}$$

Where we've used the handedness flips a charge conjugation entails, at last we now have:

$$\mathcal{L} = i\bar{\chi}\partial\!\!\!/\chi + i\bar{\omega}\partial\!\!\!/\omega - m(\bar{\chi}\omega + \bar{\omega}\chi) - M\bar{\chi}\chi \tag{2.81}$$

Now to determine the mass eigenstates we'll re-write this equation into the form

$$\mathcal{L} = i\bar{\chi}\partial\!\!\!/\chi + i\bar{\omega}\partial\!\!\!/\omega - \begin{pmatrix} \bar{\chi} & \bar{\omega} \end{pmatrix} \cdot \begin{pmatrix} M & m \\ m & 0 \end{pmatrix} \cdot \begin{pmatrix} \chi \\ \omega \end{pmatrix} \tag{2.82}$$

lets now find the eigenvalues:

$$\begin{vmatrix} M - \lambda & m \\ m & -\lambda \end{vmatrix} = (\lambda - M)\lambda - m^2 = 0 \implies \lambda_\pm = \frac{M \pm \sqrt{M^2 + 4m^2}}{2} \tag{2.83}$$

i.e

$$\lambda_\pm = \frac{M}{2}\left(1 \pm \sqrt{1 + 4m^2/M^2}\right) \tag{2.84}$$

Now we'll determine the eigenvectors:

$$\begin{bmatrix} M - \lambda_\pm & m \\ m & -\lambda_\pm \end{bmatrix} \begin{pmatrix} x_\pm \\ y_\pm \end{pmatrix} = \vec{0} \tag{2.85}$$

this gives

$$Mx_\pm - \lambda_\pm x_\pm + my_\pm = 0 \tag{2.86}$$

$$mx_\pm - \lambda_\pm y_\pm = 0 \implies \frac{mx_\pm}{\lambda_\pm} = y_\pm \tag{2.87}$$

inserting the second equation in the first we get:

$$Mx_\pm - \lambda_\pm x_\pm + m\frac{mx_\pm}{\lambda_\pm} = 0 = M\lambda_\pm x_\pm - \lambda_\pm^2 x_\pm + m^2 x_\pm \tag{2.88}$$

$$= x_\pm(\lambda_\pm^2 - M\lambda_\pm + m^2) \tag{2.89}$$

which is true for every $x_\pm$ (see equation 2.83) i.e we can freely choose $x_\pm$ so let's opt for $x_\pm^2 + y_\pm^2 = 1$:

$$x_\pm^2\left(1 + \frac{m^2}{\lambda_\pm^2}\right) = 1 \implies x_\pm^2 = \frac{1}{1 + \frac{m^2}{\lambda_\pm^2}} \implies x_\pm = \frac{\lambda_\pm}{\sqrt{\lambda_\pm^2 + m^2}} \tag{2.90}$$

$$\& \quad y_\pm = \frac{m}{\sqrt{\lambda_\pm^2 + m^2}} \tag{2.91}$$

And thus, summing up, we get the eigenvectors $\phi_\pm$ with eigenvalues $m_\pm$:

$$\phi_\pm := \begin{pmatrix} x_\pm \\ y_\pm \end{pmatrix} = \begin{pmatrix} \frac{\lambda_\pm}{\sqrt{\lambda_\pm^2 + m^2}} \\ \frac{m}{\sqrt{\lambda_\pm^2 + m^2}} \end{pmatrix} \quad \text{and} \quad m_\pm := \lambda_\pm = \frac{M}{2}\left(1 \pm \sqrt{1 + 4m^2/M^2}\right) \tag{2.92}$$

Now we'll consider the limit $M \gg m$:

$$m_\pm = \frac{M}{2}\left(1 \pm \sqrt{1 + 4m^2/M^2}\right) \approx \frac{M}{2}\left(1 \pm 1 \pm \frac{2m^2}{M^2}\right) \tag{2.93}$$

Which gives:

$$m_+ \approx M \tag{2.94}$$

$$m_- \approx -\frac{m^2}{M} \tag{2.95}$$

and:

$$\phi_+ \approx \begin{pmatrix} \frac{M}{M} \\ \frac{m}{M} \end{pmatrix} = \begin{pmatrix} 1 \\ m/M \end{pmatrix} \tag{2.96}$$

$$\phi_- \approx \begin{pmatrix} -\frac{m}{M} \\ \frac{m}{m} \end{pmatrix} = \begin{pmatrix} -m/M \\ 1 \end{pmatrix} \tag{2.97}$$

i.e, in the χ, ω basis:

$$m_+ \approx M \quad \text{with eigenstate} \quad \chi + \frac{m}{M}\omega \tag{2.98}$$

$$m_- \approx -\frac{m^2}{M} \quad \text{with eigenstate} \quad \omega - \frac{m}{M}\chi \tag{2.99}$$

$$\tag{2.100}$$

This is what's called the See-Saw mechanism, it's both a theory of giving mass to neutrinos and explaining their small mass. For a certain m if we choose a big M we'll get a big m_+ and small m_- (and vice versa). We also see that there's only a very small mixing of states, i.e the m_- mass state is almost purely ω (and m_+ almost purely χ). The parameter m in the original matrix is forbidden by electroweak gauge symmetry, and can only appear after the symmetry has been spontaneous broken by a Higgs mechanism; for this reason a good estimate of the order of m is the vaccuum expectation energy: $m \approx v = 246 \approx 10^2 \text{GeV}$. In grand unified theories it's theorised that $M \approx 10^{15} \text{GeV}$ after symmetry breaking, using these values we get

$$m_- \approx 10^{-11} \text{GeV} \approx 10^{-2} \text{eV} \tag{2.101}$$

which seems [1] to be a reasonable order of magnitude estimate for the observed neutrino mass. This mechanism would also lead to supermassive neutrinos, which are a possible dark matter candidate.

2.2.3 Majorana fermions

A theory that's also quite interesting is that neutrinos are majorana, a dirac fermion has the following density:

$$\mathcal{L} = i\bar{\psi}\partial\!\!\!/\psi - m\bar{\psi}\psi \tag{2.102}$$

$$= i\bar{\psi}_L \partial\!\!\!/\psi_L + i\bar{\psi}_R \partial\!\!\!/\psi_R - m\bar{\psi}_R\psi_L - m\bar{\psi}_L\psi_R \tag{2.103}$$

Now assume that we only have right-handed particles:

$$\mathcal{L} = i\bar{\psi}_R \not{\partial} \psi_R - \frac{M}{2} \bar{\psi}_R \psi_{Rc} - \frac{M}{2} \bar{\psi}_{Rc} \psi_R \tag{2.104}$$

A majorana fermion is a fermion which is it's own anti-particle, i.e:

$$\chi = \frac{1}{\sqrt{2}} (\psi_R + \psi_{Rc}) = \chi_c \tag{2.105}$$

With this we have that

$$\bar{\chi}\chi = \frac{1}{2} (\bar{\psi}_R \psi_{Rc} + \bar{\psi}_{Rc} \psi_R) \tag{2.106}$$

Which we can recognize in 2.104 and

$$\bar{\chi}\not{\partial}\chi = \frac{1}{2}(\bar{\psi}_R + \bar{\psi}_{Rc})\not{\partial}(\psi_R + \psi_{Rc}) \tag{2.107}$$

$$= \frac{1}{2}\bar{\psi}_R \not{\partial} \psi_R + \frac{1}{2}\bar{\psi}_{Rc} \not{\partial} \psi_{Rc} \tag{2.108}$$

$$= \bar{\psi}_R \not{\partial} \psi_R \tag{2.109}$$

where we've used integration by parts at the end, with these we can re-write 2.104 as:

$$\mathcal{L} = i\bar{\chi}\not{\partial}\chi - M\bar{\chi}\chi \tag{2.110}$$

Thus arriving at a density for Majorana fermions with mass M, a possible detection mechanism to find out if neutrinos are Majorana is "Neutrinoless double beta decay":

Figure 2.1: normal and neutrinoless double beta decay

This is (at the time of writing) actively investigated.

2.3 Why study neutrinos?

Neutrinos are ideal messengers to identify the UHE (Ultra High Energy) sources in the universe. Unlike cosmic rays, which are deflected by magnetic fields and interact with matter and radiation on their way to us, neutrinos point back to sources and can reach Earth unperturbed from the most distant corners of the universe. Neutrinos can be generated in 2 ways: either they're generated in interactions at the sources, termed *astrophysical neutrinos*. Or they're created through the interaction of ultra-high energy cosmic rays during propagation with the cosmic microwave or other photon backgrounds termed *cosmogenic neutrinos*.

2.3.1 astrophysical neutrinos: general

As cosmic rays get accelerated they will occasionally interact with matter and photon fields near the source. These will then produce new particles, of which the most common is pions due to their low mass (a lot of available phase space). As seen in chapter 2.1.3 pions can decay into neutrino's as follows:

$$\pi^- \rightarrow \mu^- + \bar{\nu}_\mu \rightarrow e^- + \bar{\nu}_e + \nu_\mu + \bar{\nu}_\mu \tag{2.111}$$

$$\pi^+ \rightarrow \mu^+ + \nu_\mu \rightarrow e^+ + \nu_e + \bar{\nu}_\mu + \nu_\mu \tag{2.112}$$

Another possibility is direct production of neutrino's at the source, of which Supernovae are a prime example:

2.3.2 Supernovae

A star starts its life as a ball of pure hydrogen. At the core, due to the gravitational pressure of the outside plasma, fusion of hydrogen into deuterium and helium happens. Thus converting mass into energy. The pressure of this energy counteracts the pressure of gravity and the star is stable.

When the hydrogen at the core runs out no more hydrogen can be fused. For stars with masses between $8M_\odot$ and $30M_\odot$ the fusion of heavier elements starts, this can't keep going on however as at some point the star starts to form the most stable element: iron. It costs
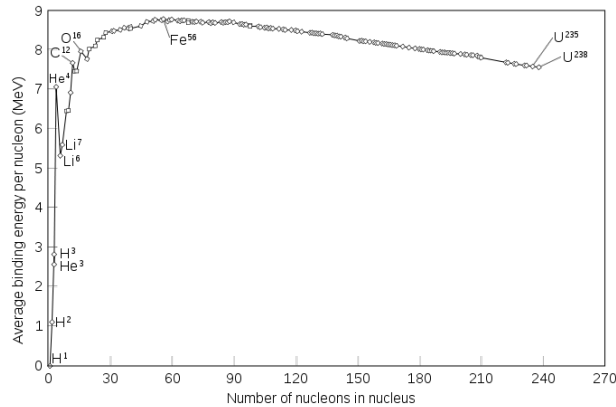
energy to both make lighter elements than iron and heavier ones. As the iron core builds up the outside pressure from the core starts to decrease as no new energy is released. This goes on until the treshold of an iron core with a mass of $1.4M_\odot$ known as the Chandrasekhar limit and the the inwards pressure becomes too large, making the electrons surrounding the iron core fuse with the protons (uud), creating neutrons (udd) and neutrino's, diagramatically:
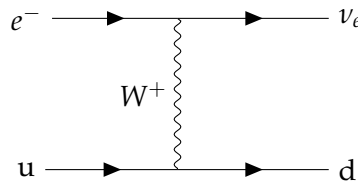
This last part happens in a split second as the collapse goes at 25% the speed of light, creating a very dense neutron star (3000km in diameter iron core to 30km in diameter neutron star) and up to 10^{52} ultra-relativistic neutrinos, carrying up to 99% of the released energy [8][4]. As

---

[4]1% is released as kinetic energy, only 0.001% as electromagnetic radiation

the density has suddenly increased so much there's a huge distance of pure vaccuum between the plasma outer layer and the (now) neutron star, this plasma starts free-falling inwards, also at 25% the speed of light whilst the neutrinos carrying tremendous amounts of energy start going outwards from the neutron stars core.

The neutrinos then collide with the plasma resulting in what we observe as a "supernova", wrongly thought of by Kepler as being a "new (nova) star" rather being a violent death of an old star.

This is quite unexpected as neutrinos rarely interact, they only do becouse the incoming plasma is so dense and due to the tremendous amount of neutrinos that collissions happen at all. Some, however, escape and will be visible on earth in our neutrino detectors $\approx$ 18h before the light escapes the exploding star.

Neutrino observatories are thus useful to know where to point our various telescopes before the supernova is actually visible in the night sky.

2.3.3 primordial neutrinos

Aside from all the previously mentioned sources, there's also a less spectacular source of neutrinos: the neutrino version of the CMB. We can estimate the temperature of the neutrinos who decoupled at the start of the universe, for this we can take a look at conservation of entropy [3] The entropy before and after decoupling is:

$$s(a_1) = \frac{2\pi^2}{45}(2 + \frac{7}{8}(2+2+3+3))T_1^3 \tag{2.113}$$

$$= \frac{2\pi^2}{45}\frac{86}{8}T_1^3 \tag{2.114}$$

$$s(a_2) = \frac{2\pi^2}{45}(2T_\gamma^3 + \frac{7}{8}(6)T_\nu^3) \tag{2.115}$$

$$\tag{2.116}$$

Conservation of entropy:

$$s(a_1)a_1^3 = s(a_2)a_2^3 \tag{2.117}$$

$$\frac{86}{8}(T_1a_1)^3 = \left(2\left(\frac{T_\gamma}{T_\nu}\right)^3 + \frac{42}{8}\right)(T_\nu a_2)^3 \tag{2.118}$$

$$\frac{86}{8} = 2\left(\frac{T_\gamma}{T_\nu}\right)^3 + \frac{42}{8} \tag{2.119}$$

$$\frac{44}{16} = \left(\frac{T_\gamma}{T_\nu}\right)^3 \tag{2.120}$$

$$\left(\frac{T_\gamma}{T_\nu}\right) = \left(\frac{11}{4}\right)^{1/3} \tag{2.121}$$

i.e

$$T_\nu = \left(\frac{4}{11}\right)^{1/3}T_\gamma \tag{2.122}$$

2.3.4 How do they fit into the full detector spectrum?

The origin of the most energetic cosmic rays is still not conclusively identified. One approach to solving this problem is *multi-messenger astrophysics*, where several types of cosmic particles are used to identify the sources of these ultra-high energy cosmic rays (UHECRs). E.g

we simultaneously measure gravitational waves (gravitons?) with the Einstein telescope, neutrino's with IceCube (or eventually RNO-G), photons with various telescopes and muons with a muon detector.

CHAPTER

3

BACKGROUND: RADIO DETECTION

For a particle shower to emit strong radio signals, two conditions have to be met:

- There needs to be a speration of positive and negative charges in the shower front

- The signals produced over the length of the shower profile need to overlap coherently.

The first item, seperation of positive and negative charges, can be caused by 2 mechanisms:

The *Askaryan* [2] effect, also known as Askaryan radiation. This is the phenomenon whereby a particle traveling faster than the phase velocity of light in a dense dielectric (such as ice) produces a shower of secondary charged particles which contains a charge anisotropy (net negative charge), this charge imbalance is a result of medium electrons either Compton scattering into the advancing shower or annihilating with shower positrons. You end up having moving charges which move faster than the speed of light in the medium, creating Cherenkov radiation.

The other possible mechanism, called *geomagnetic emission* is the seperation of charges by the Lorentz force from the geomagnetic field, however, because of its relatively high density, in ice the Askaryan effect is dominant. It's possible to distinguish between the two with polarization as with Askaryan emission, the light is polarized in the radial direction towards the shower axis contrary to geomagnetic emission where it's polarized in the Lorentz force direction.

In the following two sections I'll quickly give a short overview of the equations of Cherenkov radiation to determine the viewing angle of an incoming neutrino particle, this is relevant to the second condition which I'll explain afterwards.[1]

---

[1]The reader who wants a thorough explanation and derivation is advised to check out *Chapter 14: Radiation by Moving Charges* from the book *Classical Electrodynamics* by Jackson.

3.1   Spectral distribution

We wish to know the emitted energy per elementary unit solid angle over a certain frequency interval for a moving charge far away from the source. For this we have that the vectorpotential **A**, defined as

$$\mathbf{B} = \nabla \times \mathbf{A} \tag{3.1}$$

takes the form

$$\mathbf{A}(\omega) = \frac{q}{4\pi\sqrt{2\pi}} \sqrt{\frac{\mu}{\epsilon}} \frac{e^{ikr}}{r} \boldsymbol{\alpha} \tag{3.2}$$

with q the charge, r the distance from the charge to the observer and

$$\boldsymbol{\alpha} = \int_{\infty}^{\infty} \boldsymbol{\beta}(t) e^{i\omega(t - \mathbf{e}_r \cdot \mathbf{r}_0(t)/c')} \mathrm{d}t \tag{3.3}$$

With $\boldsymbol{\beta} := \mathbf{u}/c'$ wherein $\mathbf{u}$ is the speed of the particle, c' is the local speed of light and the integration is along the path of the moving charged particle. The energy emitted per unit solid angle is given by

$$\frac{\mathrm{d}\mathscr{P}}{\mathrm{d}\Omega} = R'^2 \mathbf{S}(t) \cdot \mathbf{n}' \tag{3.4}$$

Defining $\mathscr{E}$ to be the time integral of this, we can reformulate this into (standard practice to integrate over the frequencies)

$$\frac{\mathrm{d}\mathscr{E}}{\mathrm{d}\Omega} = r^2 \int_{\infty}^{\infty} \mathrm{d}\omega (\mathbf{E}(\omega) \times \mathbf{H}(-\omega)) \cdot \mathbf{e}_r = \int_0^{\infty} \frac{\mathrm{d}^2 \mathscr{J}(\omega)}{\mathrm{d}\omega \mathrm{d}\Omega} \tag{3.5}$$

i.e $\frac{\mathrm{d}^2 \mathscr{J}}{\mathrm{d}\omega \mathrm{d}\Omega}$ is the energy radiated per elementary unit solid angle and per elementary unit frequency interval, re-writing gives

$$\frac{\mathrm{d}^2 \mathscr{J}(\omega)}{\mathrm{d}\omega \mathrm{d}\Omega} = 2r^2 \Re\{\mathbf{E}(\omega) \times \mathbf{H}^*(\omega)\} \cdot \mathbf{e}_r \tag{3.6}$$

up to $\mathcal{O}(r^{-2})$ we get

$$\frac{\mathrm{d}^2 \mathscr{J}(\omega)}{\mathrm{d}\omega \mathrm{d}\Omega} = \frac{q^2 \omega^2}{16\pi^3} \sqrt{\frac{\mu}{\epsilon}} |\mathbf{e}_r \times (\mathbf{e}_r \times \boldsymbol{\alpha})|^2 \tag{3.7}$$

3.2   Cherenkov radiation

Cherenkov radiation is like the elektromagnetic equivalent of a sonic boom, a sonic boom happens when something goes faster than the sounds speed in the medium; A particle emits Cherenkov radiation if it goes faster than the light speed in the medium. Choosing the particle trajectory to lie along the z axis we can approximate equation 3.7 as

$$\frac{\mathrm{d}^2 \mathscr{J}(\omega)}{\mathrm{d}\omega \mathrm{d}\Omega} = \frac{q^2}{4\pi} \sqrt{\frac{\mu}{\epsilon}} \beta^2 \omega^2 \delta^2 [\omega(1 - \beta \mathbf{e}_r \cdot \mathbf{e}_z)] |\mathbf{e}_r \times \mathbf{e}_z|^2 \tag{3.8}$$

or, in spherical coordinates, $1 - \beta \mathbf{e}_r \cdot \mathbf{e}_z = 1 - \beta \cos(\theta_c)$ in the delta function. We thus only expect radiation if

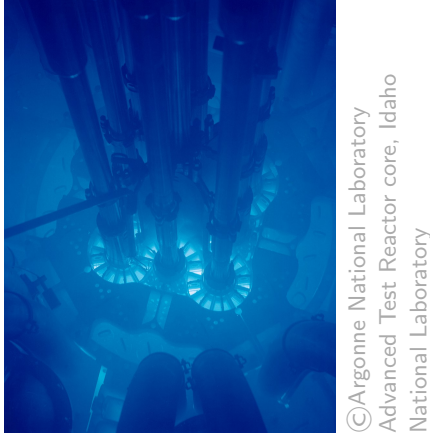$$\cos(\theta_c) = \frac{1}{\beta} = \frac{c'}{u} = \frac{c}{n} \cdot \frac{1}{u} \tag{3.9}$$

Figure 3.1: Cherenkov radiation in a nuclear reactor

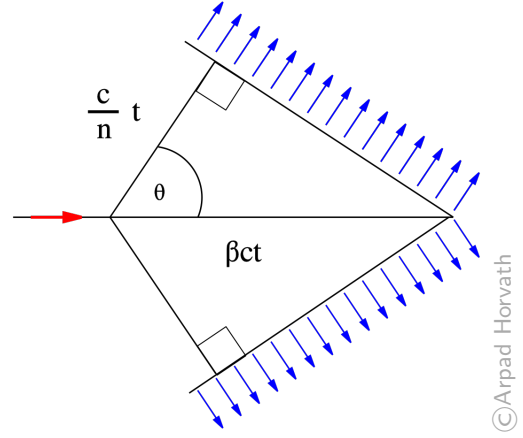

Figure 3.2: Diagrammatic representation of Cherenkov radiation

I.e if $u > \frac{c}{n}$ with n the index of refraction, Cherenkov radiation will be emitted along a cone surface with half angle $\frac{\pi}{2} - \theta_c$ as illustrated in figure 3.2. Integrating equation 3.8 over the solid angle and formally deviding by the time interval we get:

$$\frac{\mathrm{d}^2 \mathscr{J}}{\mathrm{d}\omega \mathrm{d}t} = \frac{q^2}{4\pi}\sqrt{\frac{\mu}{\epsilon}}\beta\omega\left(1 - \frac{1}{\beta^2}\right) \tag{3.10}$$

We see that the energy is proportional to ω, so we expect that most radiation will be emitted "in blue", as seen in figure 3.1. For ice the index of refraction is roughly 1.75, so we expect an ultra-relativistic particle to produce the most radiation at around 55° opening as $\cos\left(\frac{1}{1.75}\right) \approx$ 55° (generally we take 56°). Now if an observer is positioned at this Cherenkov angle all radio emission produced during the shower development reaches him/it at the same time, leading to constructive interference, hence the second condition (coherent overlap) is satisfied in ice for signals at $\approx 56°$

3.3 Reconstruction

It can pose a challenge to reconstruct the radio signals produced by the Cherenkov radiation as they are often obscured by background noise. A solution used in RadioReco is Information Field Theory (IFT) implemented in RadioReco by Welling et al. [10] which uses Bayesian inference to calculate the most likely radio signal, given recorded data. The full reconstruction will then work as follows: events and their propagation are generated in a monte-carlo simulation using NuRadioMC [6] [5], how the detector signals would look like is then simulated with RadioReco and saved in a database. If we then detect a neutrino event in the real detector it can be compared to the database, thus finding the origin.

CHAPTER

4

THE DETECTOR

Both cosmic ray and neutrino detectors face the same main problem at the highest energies: the steeply falling flux (as can be seen on figure 4.1) requires large effective areas, which leads to the construction of neutrino detectors with volumes on the cubic kilometer scale: IceCube. As we wish to detect neutrino's with even higher energies we turn to look at an array of detectors spanning multiple cubic kilometers: RNO-G.

One such detector is illustrated in figure 4.2.

The deep component of the detector can be split up in three parts: Two *helper strings*, one *power string* and the surface components. The helper strings are the 2 vertical cables shown on the right of the figure and each one houses 2 vertically polarized antennas (Vpols), one quadslot antenna for the horizontal polarization component (Hpol) and one radio pulser on each helper string which can be used to generate calibration signals.

The power string (the leftmost vertical cable) is more densely instrumented: At the bottom it houses a set of four Vpol and two Hpol antennas with a spacing of 1m and further up the string, with a spacing of 20m are three more Vpol antennas.

The signal from each of these antennae are fed into a low-noise amplifier directly above it, from there the signal is send to the data acquisition (DAQ) system at the surface via a Radio Frequency over Fiber (RFoF) cable. There it's again amplified, digitized and saved onto an SD card. This data is then transmitted via a Long Term Evolution (LTE) telecommunications network to a local server[1], from where it is sent via a sattelite link.

There are solar panels as a power source who charge up battery banks, but as there is't enough light during the Greenland winters, there're plans to build wind turbines (with the problem being the possibly detectable RF noise the 'engine' produces)

---

[1]There is additionally a Long Range Wide Area Network (LoRaWAN) antenna as backup in case of problems with the LTE network
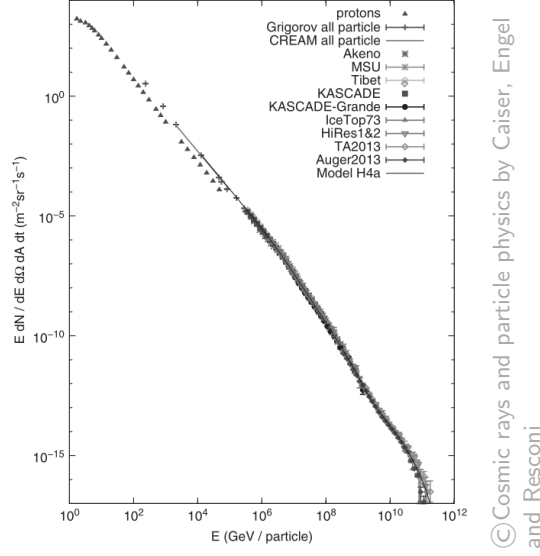
Figure 4.1: Falling cosmic ray flux with energy

The radio signal from a neutrino often travels along both direct and refracted paths (designated DnR) to the deep array, this happens because the upper ice layer is a non-uniform medium where the signal trajectory is bent, as illustrated by a simulation in figure 4.3.

This double pulse characteristic would be a smoking-gun signature of an in-ice source. The two helper strings are needed for a full direction reconstruction. Three independent measurements are needed for azimuthal information, which is provided by the Vpol (Vertical polarization) antennas and placing the Hpol (Horizontal polarization) antennas at different depths on every string, both zentih and azimuth information will be provided for those signals. The helper strings' calibration pulsers, as well as one on the surface, will ensure regular monitoring of the performance of the station and provide information useful for precise calibration of the antenna geometry.

The plan is to construct these detectors in an array as shown in figure 4.4, note that all the individual detectors are named after various species living in greenland (in the native tongue).

Christoph Welling did an investigation into energy reconstruction from the received signals [11] for air showers in one single station (as the RNO-G stations are so far apart this is the case here aswell) and he noticed that it is nescessary to know if the detector who observes an event falls inside or outside the Cherenkov cone to accurately reconstruct the primary particle energy as most over-estimated energies in his simulations are caused by events viewed from within the Cherenkov ring being mistaken for events outside of it. He went on to show that, if we somehow know if the shower was seen from inside or outside the ring from some extra source, that most outliers in the energy disappeared. It is shown by Hiller et al. [7] that the combination of a muon detector with the radio detector might make the issue of confusion between being within or outside of the Cherenkov-ring disappear. Because of this the RNO-G stations are fitted with surface Log Periodic Dipole Antennas (LPDA), capable of detecting muons. Note that this is for air showers, the radio signal from neutrinos show additional complexities.
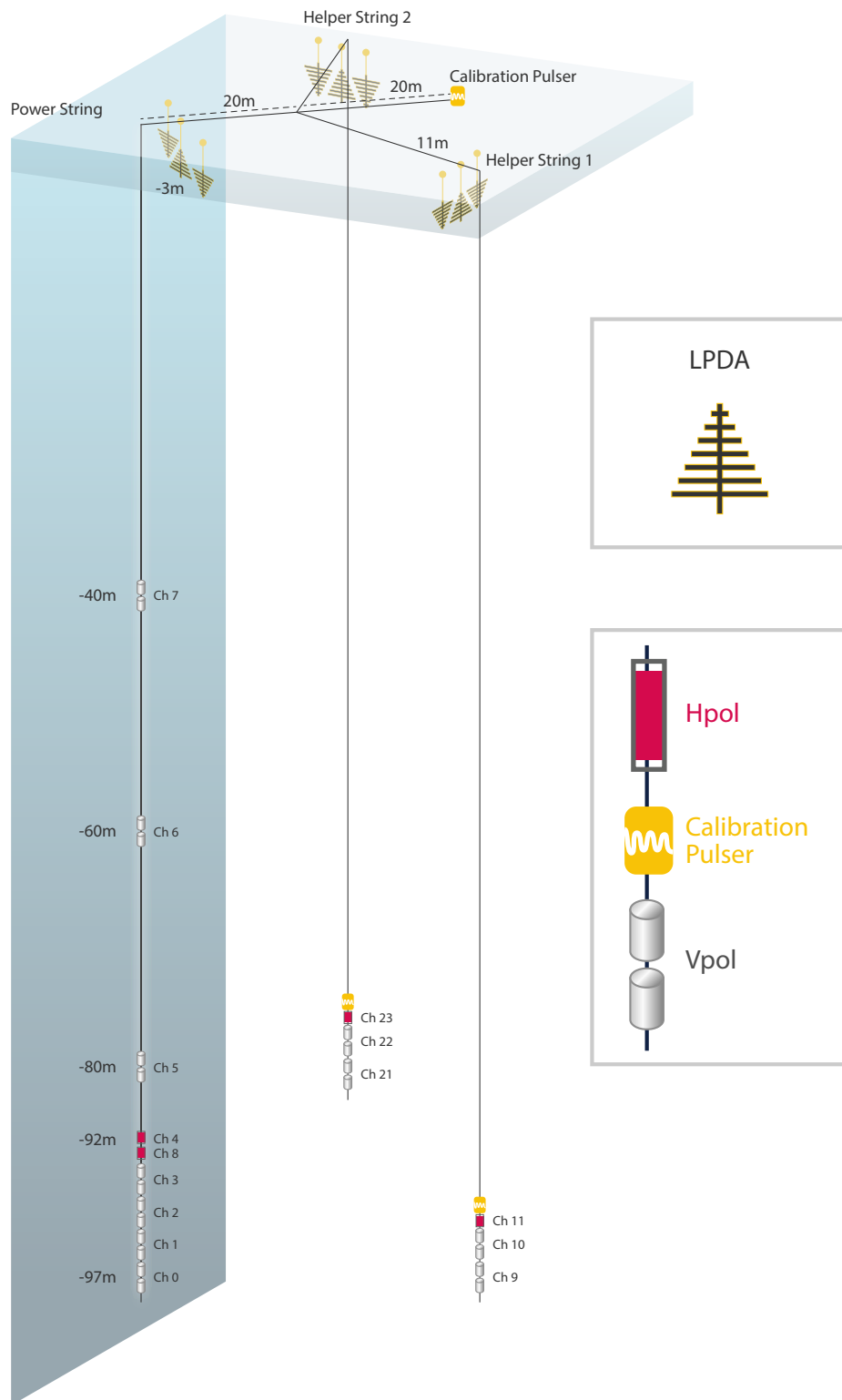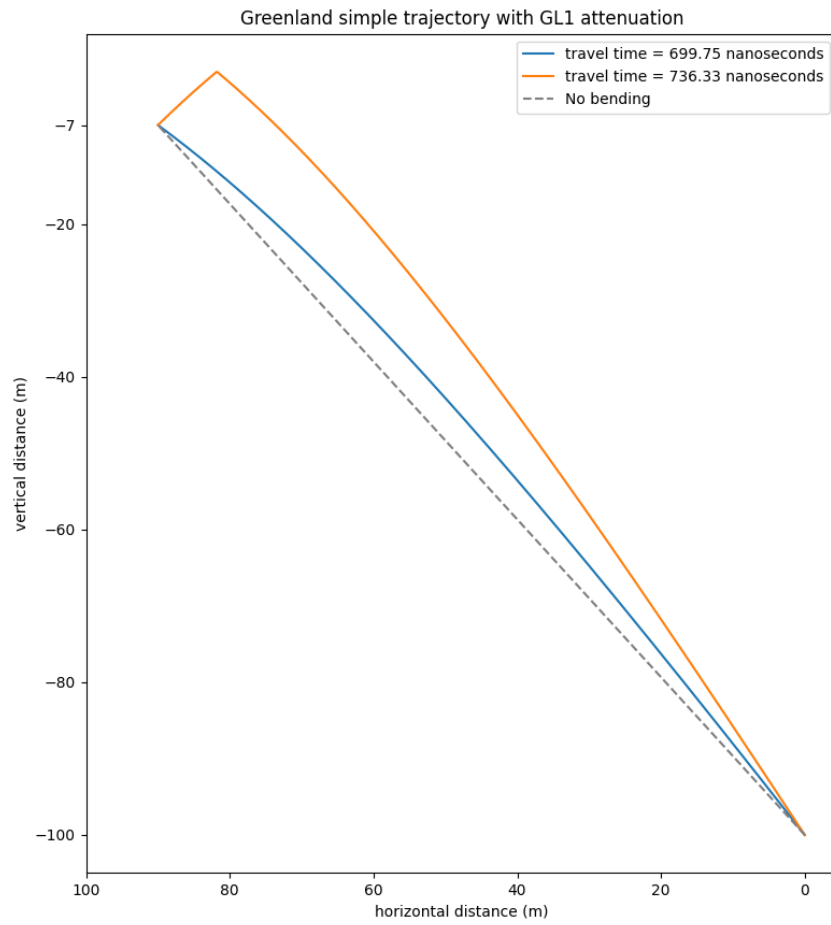
Figure 4.2: illustration of the detector

Figure 4.3: illustration of a neutrino signal path, the neutrino interaction being located at (0,-100) and the detector at (90,-7)

Figure 4.4: map of the station

CHAPTER

5

HYBRID RAY TRACER

5.1 Introduction

It has become apparent [citation needed] that complex ice models will be nescessary moving forward as the exponential ice model fails to fit the density curve. The ideal software for radio wave propagation through ice is radiopropa [12], but due to the way it works you'll have to know the start point , the end point and the launch angle of your ray to work out the path. With the exponential model the launch angle is known from solving a simple equation. However for a more difficult ice model the launch angle can't be know a priori. Work has been done on this by B. Oeyen et al. [9], where they created a ray tracer which iteratively finds the solution, called the "iterative ray tracer". The full explanation of how their algorithm works can be found in the mentioned paper. This is however a sub-optimal solution in python as an optimalisation library will generally work faster, work had been done on trying to implement such an algorithm but this attempt failed. As I saw this work I had an idea to combine the iterative ray tracer and the code using the optimisation libraries (a so called "minimizer"), to come up with the algorithm that will be discussed in this chapter: The hybrid ray tracer, in the source code called the "hybrid minimizer".

It succeeds in more rapidly tracing the path from the event to the detector, is more accurate and also arrives closer to the detector as the final result is not limited by the final drawn sphere size but by a given tolerence.

5.2 How it works

The hybrid minimizer can be seen as an extension of the iterative raytracer, it checks after the first loop (as explained in the paper by B. Oeyen et al. [9]) if there are 2 distinct launch regions, if this is the case it breaks out of the loop as is visually explained using a modified version of B. Oeyen et al. their figure in the top part of figure 5.1. It then goes on to use the scipy.optimize.minimize module to find the solutions in the respective angle intervals as shown in the bottom part of figure 5.1 (minimizing Δz). If it doesn't find 2 distinct regions after the first loop, it falls back on the iterative ray tracer.
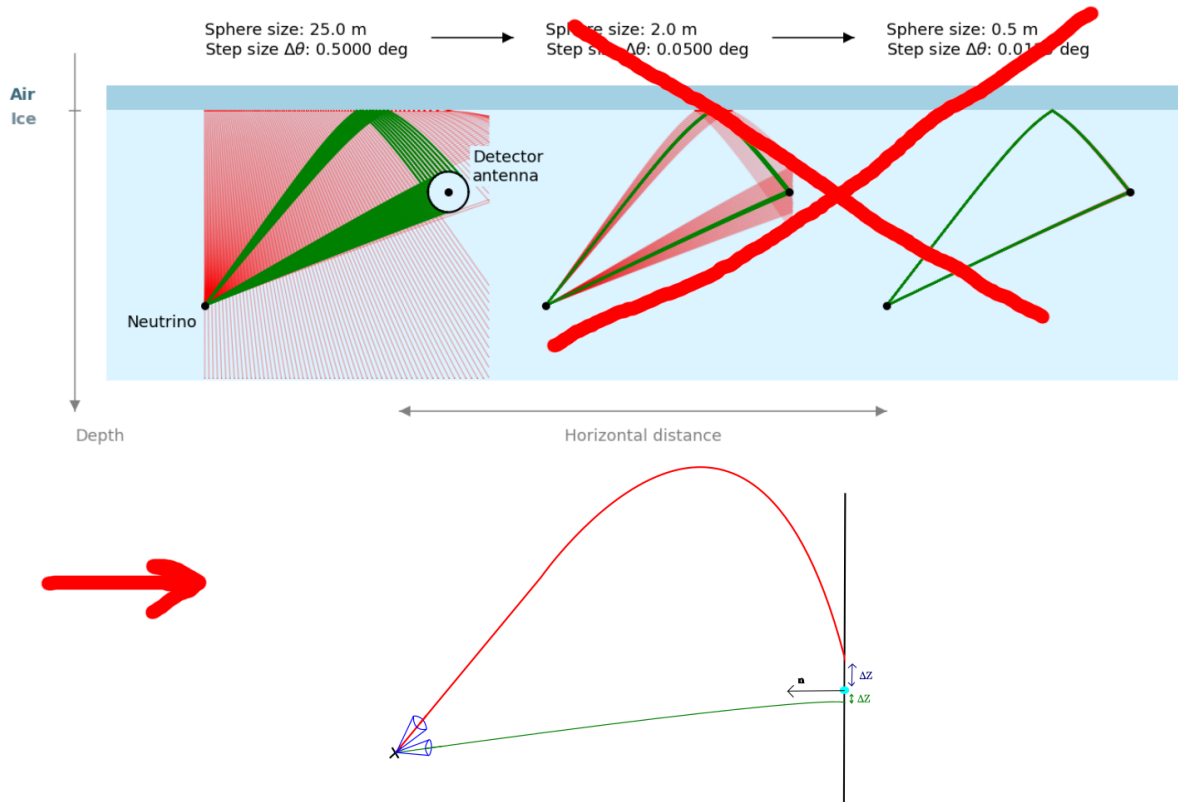
Figure 5.1: explanation of the hybrid method

5.3   random number generator

To test the hybrid minimizer the numpy random module was used to generate random coördinates, the considered square (as there is only a z component to the ice model the 3D problem is essentially only a 2D problem) is x:0.1km,4km and z:-0.1km,-3km.[1]

5.4   Performance Optimalisation

5.4.1   Length of the normal vector

As visually explained in figure 5.2, the size of the normal vector seems to influence how big the ray tracer's step size is taken close to the detector. This thus influences the convergence and time taken. The results of varying this are shown in figures 5.5 and 5.6. Looking at these figures the first optimization conclusion is as expected: take the normal vector length to be 1 meter.

5.4.2   ztol

We'll now change the tolerence on the vertical distance away from the detector which is deemed accepted i.e in figure 5.2 if Δz is below this threshold it's accepted. The results are shown in figures 5.7 and 5.8. From which we can conclude the second optimization conclusion: take ztol to be 0.05 m.

---

[1]This start at 100m depth was to get around issues concerning events that won't even trigger in a full simulation
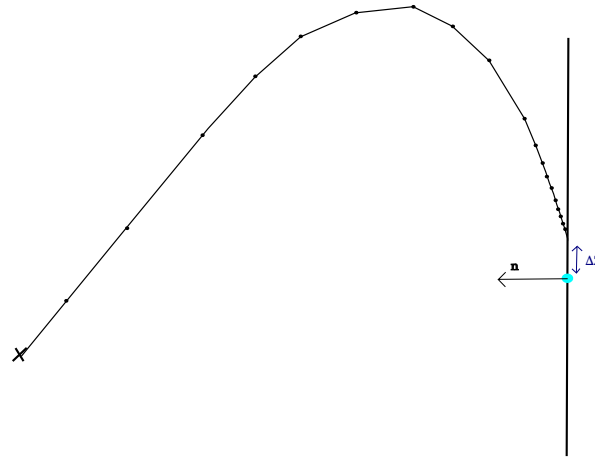
Figure 5.2: how normal vector size influences the stepsize
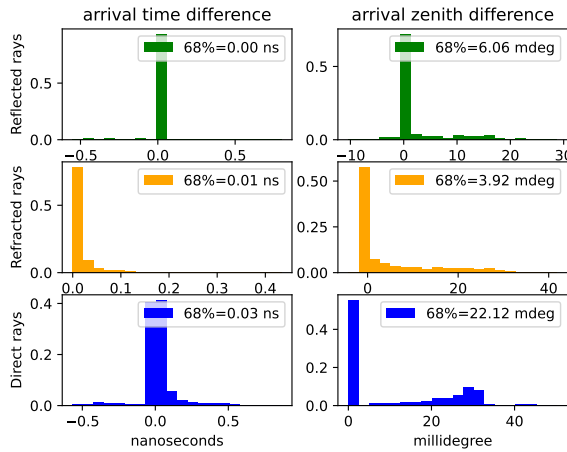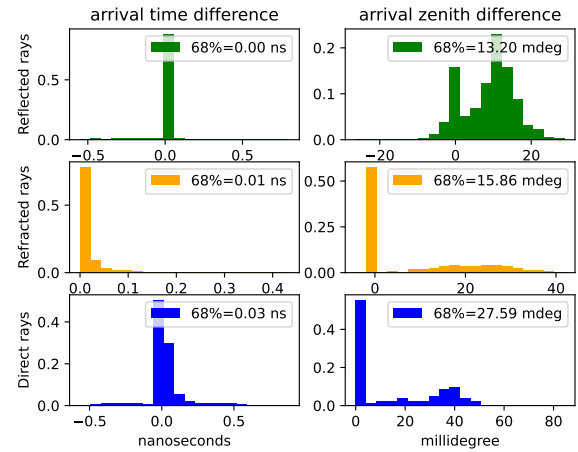

Figure 5.3: Hybrid

Figure 5.4: Iterative

5.4.3 Sphere Size & Step Size

As explained in Oeyen et al.'s work, the initial rays are sent out in steps of a certain angle and with a sphere around the detector (as can also be seen at the top of figure 5.1, but for clarification I again refer to their paper). The sphere size and step size weren't jet optimized. But as this is the slowest step in the hybrid ray tracer this was optimized here (only the initial sphere and step size as those are relevant for the hybrid raytracer) as seen in figures 5.9 and 5.10.
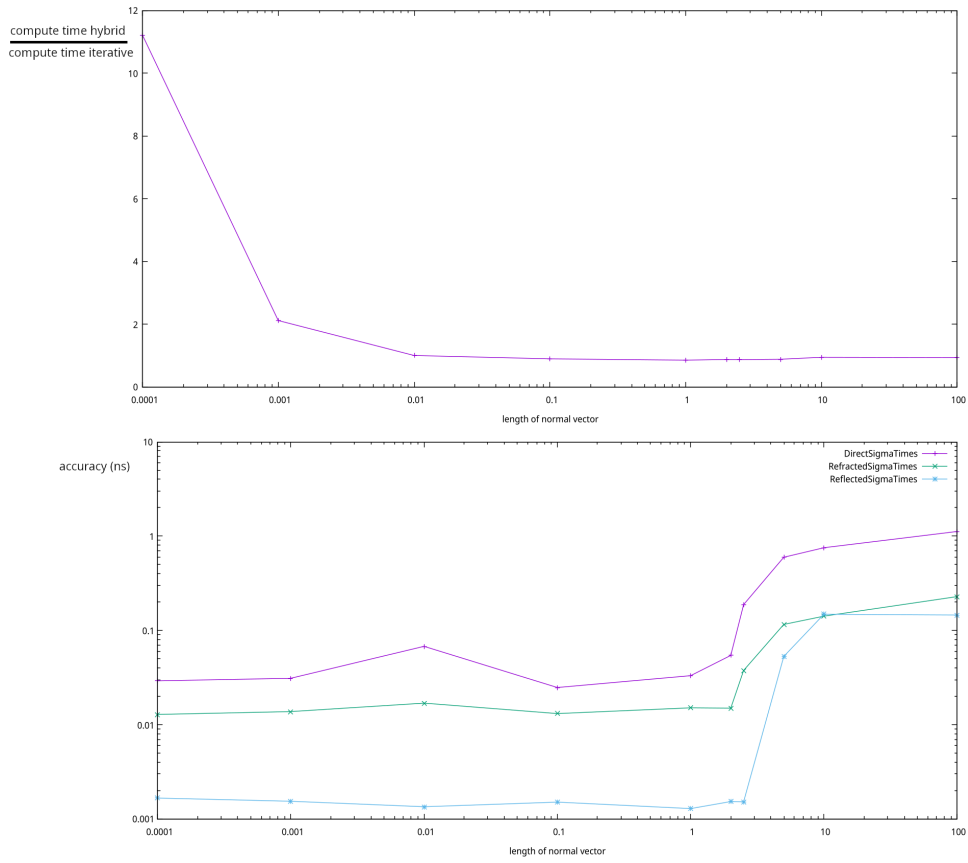
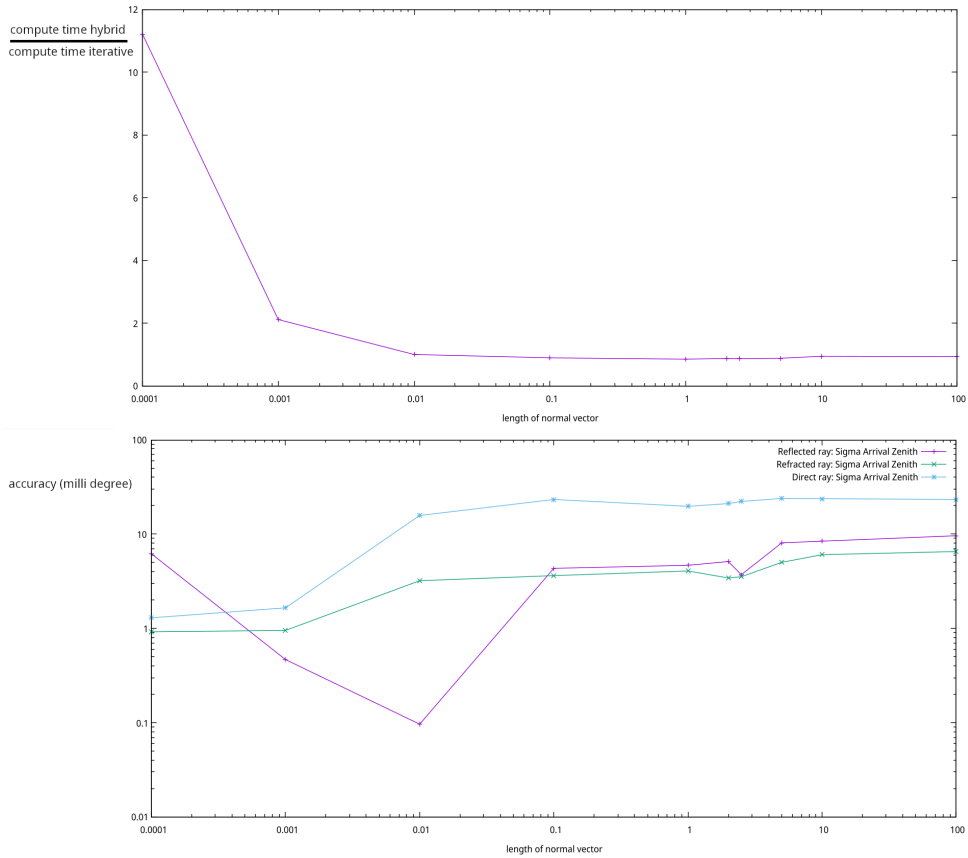Figure 5.5: influence of the length of the normal vector

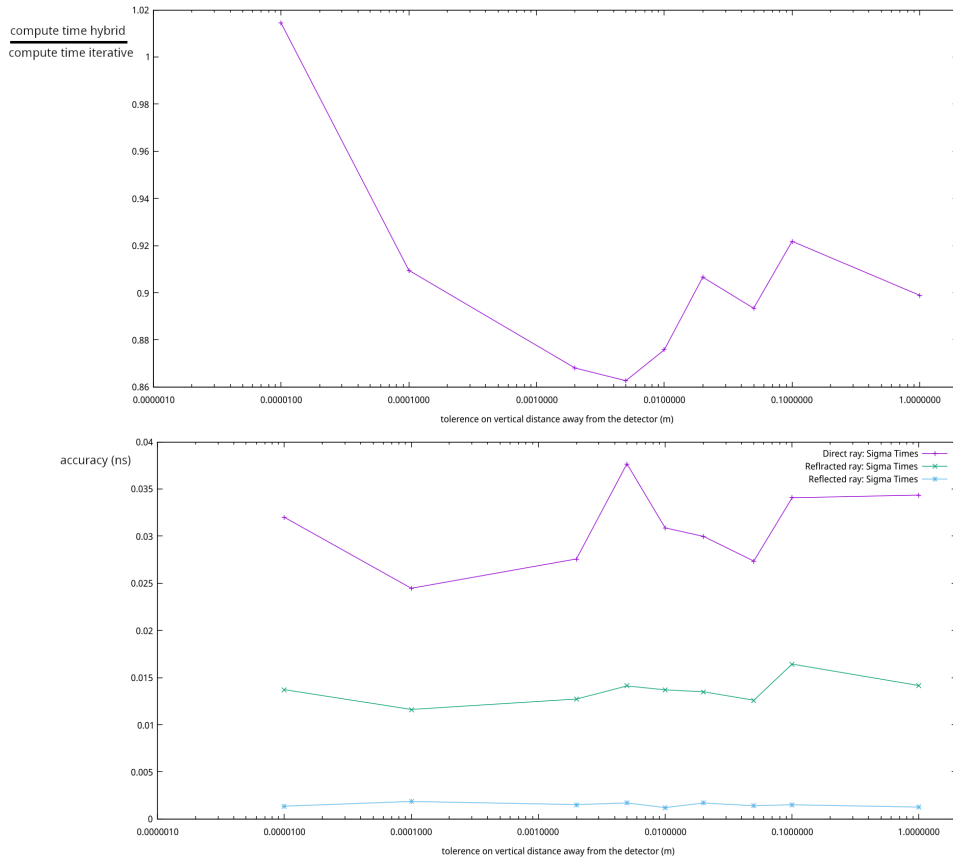Figure 5.6: influence of the length of the normal vector

29

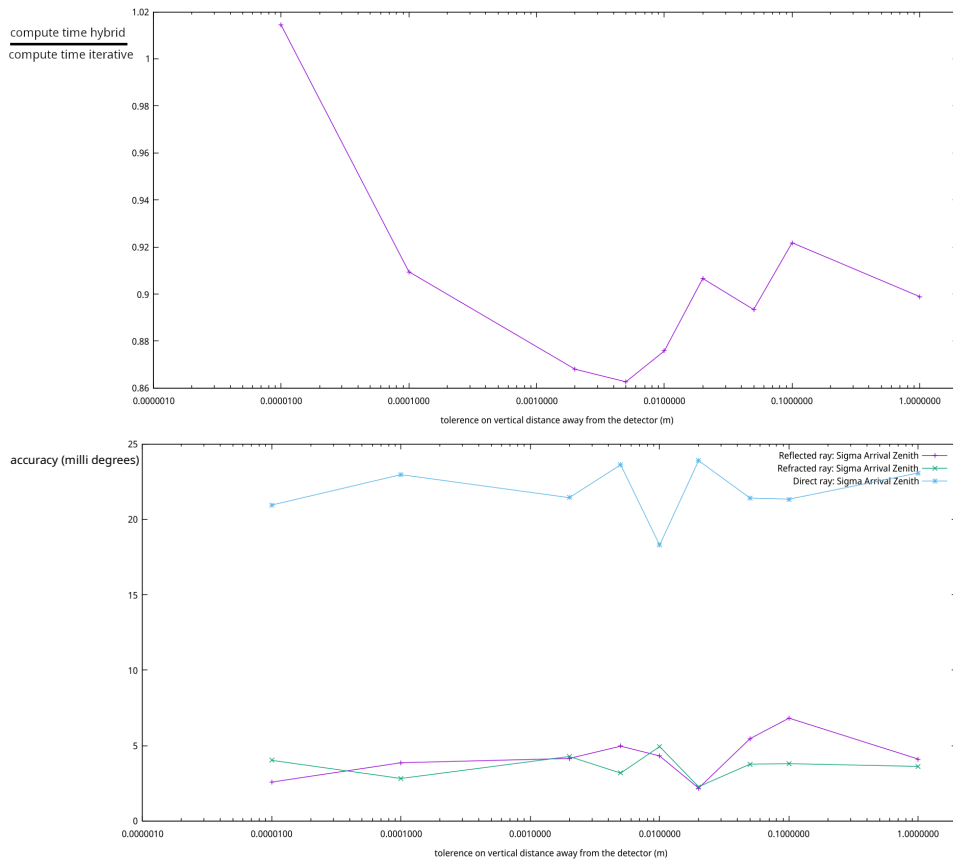Figure 5.7: influence of the tolerence on vertical distance

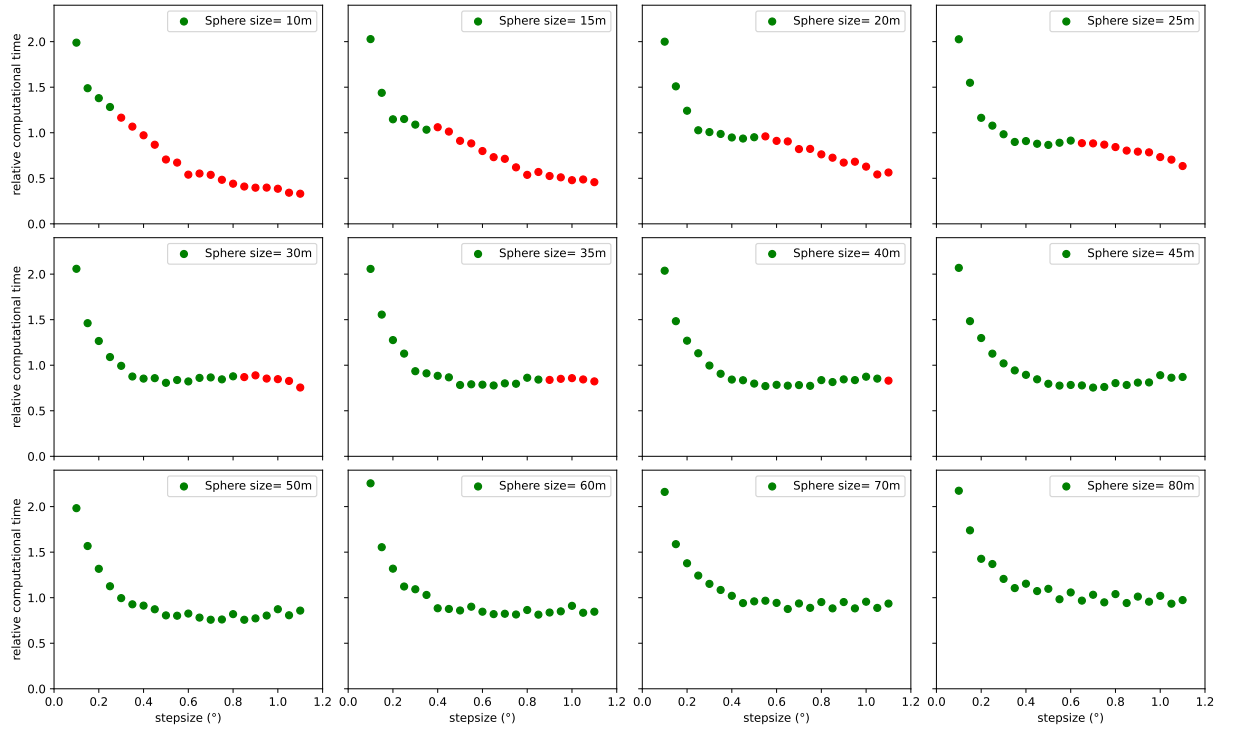Figure 5.8: influence of the tolerence on vertical distance

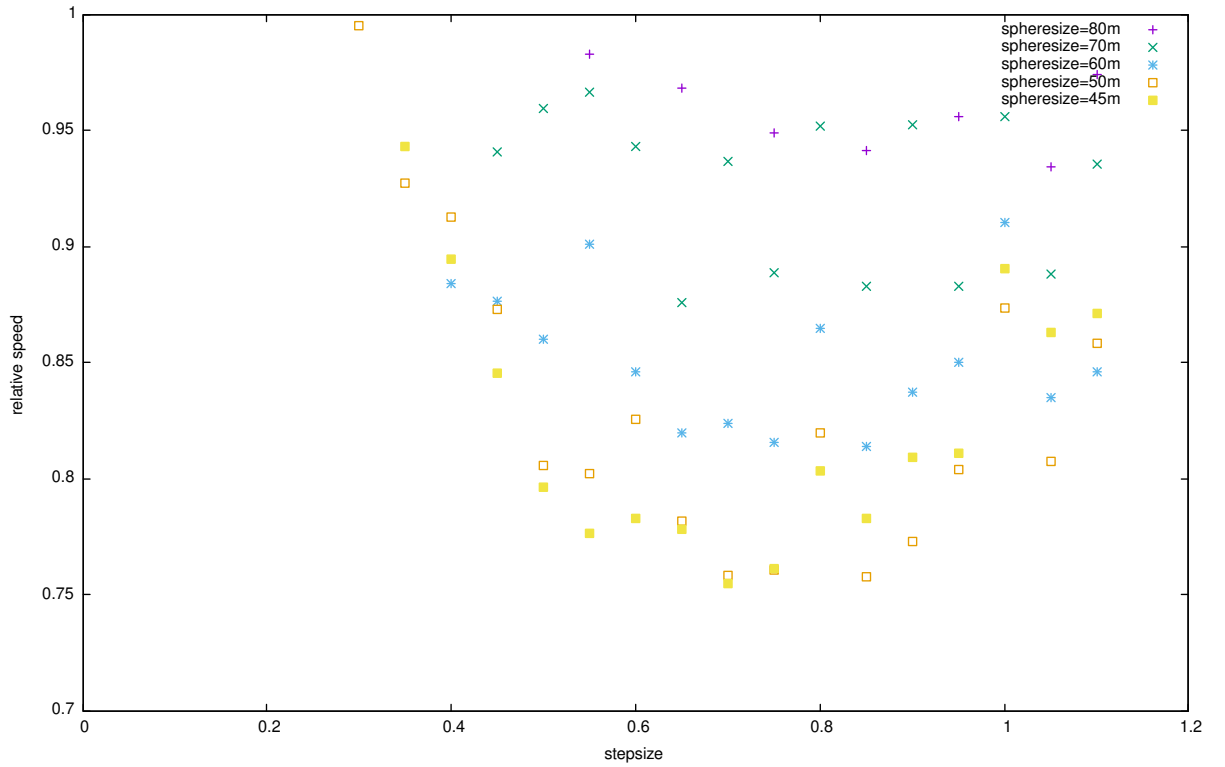Figure 5.9: Variation in Sphere and angle step size with report on relative time.

Figure 5.10: Green values in variation in sphere and angle step size with report on relative time.

BIBLIOGRAPHY

[1] M. Aker, A. Beglarian, J. Behrens, A. Berlev, U. Besserer, B. Bieringer, F. Block, S. Bobien, M. Böttcher, Bornschein, et al. Direct neutrino-mass measurement with sub-electronvolt sensitivity.

[2] G A Askaryan. Excess negative charge of an electron-photon shower and the coherent radio emission from it. Zhur. Eksptl'. i Teoret. Fiz., 41, 8 1961.

[3] Scott Dodelson. Modern Cosmology. Academic Press, Amsterdam, 2003.

[4] K. Eguchi, S. Enomoto, K. Furuno, J. Goldman, H. Hanada, H. Ikeda, K. Ikeda, K. Inoue, et al. 90(2), jan 2003.

[5] C. Glaser, D. García-Fernández, A. Nelles, J. Alvarez-Muñiz, S. W. Barwick, D. Z. Besson, B. A. Clark, A. Connolly, C. Deaconu, K. D. de Vries, J. C. Hanson, B. Hokanson-Fasig, R. Lahmann, U. Latif, S. A. Kleinfelder, C. Persichilli, Y. Pan, C. Pfendner, I. Plaisier, D. Seckel, J. Torres, S. Toscano, N. van Eijndhoven, A. Vieregg, C. Welling, T. Winchen, and S. A. Wissel. NuRadioMC: simulating the radio emission of neutrinos from interaction to detector. The European Physical Journal C, 80(2), jan 2020.

[6] Christian Glaser, Anna Nelles, Ilse Plaisier, Christoph Welling, Steven W. Barwick, Daniel García-Fernández, Geoffrey Gaswint, Robert Lahmann, and Christopher Persichilli. NuRadioReco: a reconstruction framework for radio neutrino detectors. The European Physical Journal C, 79(6), jun 2019.

[7] R. Hiller, P. A. Bezyazeekov, N. M. Budnev, et al. Tunka-rex: energy reconstruction with a single antenna station. EPJ Web of Conferences, 135:01004, 2017.

[8] Tobias Melson, Hans-Thomas Janka, Robert Bollig, Florian Hanke, Andreas Marek, and Bernhard Müller. Neutrino-driven explosion of a 20 solar-mass star in three dimensions enabled by strange-quark contributions to neutrino–nucleon scattering. The Astrophysical Journal Letters, 808(2):L42, jul 2015.

[9] B. Oeyen, I. Plaisier, A. Nelles, C. Glaser, and T. Winchen. Effects of firn ice models on radio neutrino simulations using a RadioPropa ray tracer. In 37th International Cosmic Ray Conference. 12-23 July 2021. Berlin, page 1027, March 2022.

[10] C. Welling, P. Frank, T. Enßlin, and A. Nelles. Reconstructing non-repeating radio pulses with information field theory. Journal of Cosmology and Astroparticle Physics, 2021(04):071, apr 2021.

[11] C. Welling, C. Glaser, and A. Nelles. Reconstructing the cosmic-ray energy from the radio signal measured in one single station. Journal of Cosmology and Astroparticle Physics, 10:075–075, oct 2019.

[12] Tobias Winchen. RadioPropa — a modular raytracer for in-matter radio propagation. EPJ Web of Conferences, 216:03002, 2019.